

Quantum orbital entanglement: A view from the extended periodic Anderson model

L. Craco

Max-Planck-Institut für Chemische Physik fester Stoffe, 01187 Dresden, Germany

(Received 5 December 2007; revised manuscript received 14 February 2008; published 17 March 2008)

In an attempt to derive the electronic structure of narrow-band systems, we extend the periodic Anderson model by exploiting the Falicov–Kimball–Hubbard interactions. The dynamical mean-field theory is used to obtain the spectral densities and self-energies of the combined model. We show that correlated orbitals become locally entangled due to composite orbital rehybridization. This many-orbital quantum phenomenon is accompanied by a continuous metal-insulator transition away from half-filling. Our results are relevant for the understanding of the role of the multiorbital Kondo screening processes in generating local orbital entanglement in Kondo systems.

DOI: [10.1103/PhysRevB.77.125122](https://doi.org/10.1103/PhysRevB.77.125122)

PACS number(s): 71.27.+a, 71.28.+d, 71.30.+h, 75.30.Mb

I. INTRODUCTION

The periodic Anderson model (PAM)¹ and the Falicov–Kimball model (FKM)² were introduced in the 1960s to explore the correlated nature of rare-earth and transition-metal compounds. In these fascinating models, there are two types of electronic states: a localized f level, which does not overlap with neighboring electronic sites, and a delocalized conduction d band. The localized f electrons in PAM strongly interact with each other via the on-site Coulomb interaction U_{ff} , which forbids double occupancy of the heavy particles, and the conduction electrons are assumed to be uncorrelated, $U_{dd}=0$. The model proposed by Falicov and Kimball is based on similar assumptions. However, in this model, U_{ff} is often set to infinity and the remaining Coulomb interaction takes place between electrons on different orbitals (U_{df}), when a conduction and a localized electron occupy the same lattice site. In PAM, the on-site hybridization V mixes the localized states with the conduction band, providing a theoretical basis for the understanding of the band-gap formation in heavy-fermion semiconductors.³

Historically, the valence fluctuation phenomenon and its relation to various limiting cases of Eq. (1) below were addressed in the early 1980s.^{4,5} We recall, for example, that the influence of the interorbital Coulomb interaction U_{df} on the electronic phase transitions in Ce- and the insulator-metal transition in Sm-based compounds were investigated within the Falicov–Kimball framework.⁶ In addition, the continuous metal-insulator transition of the spinless FKM accounts for several physical responses in YbInCu₄ (Ref. 7) and EuNi₂(Si_{1-x}Ge_x)₂ (Ref. 8) compounds. The regular PAM, on the other hand, has been used to describe electronic and magnetic properties of Kondo insulators.⁹ In its canonical form, it explains, for example, the heavy-electron masses found in 4*f* and 5*f* compounds¹⁰ (heavy fermions) and the nature of their insulating state, which is attributed to the df hybridization V . Indeed, it is widely believed that in Kondo insulators, the hybridization V (with or without \mathbf{k} dependence) is responsible for the band-gap formation in the one-particle spectral function in a way similar to what is seen in normal semiconductors. However, the charge gap, which is of the order of V in the free electron limit, is smeared to a pseudogap by strong f -electron spin fluctuations in the Kondo insulating regime.

In recent years, various theoretical works have dealt with the formation of spin and orbital *entanglement* in PAM and Kondo-based models.^{11,12} Of great interest here are real solid-state devices, where the entanglement between magnetic impurities is linked to orbital degrees of freedom of delocalized electronic carriers.¹³ On the fundamental side, it is now well accepted that entanglement (or the quantum-mechanical correlation between subelectronic systems) plays an important role in a number of quantum information schemes.¹⁴ Moreover, due to its intrinsic quantum nature, this generic effect might be useful to identify quantum phase transitions (QPTs) in correlated fermionic systems.¹⁵ We recall that it is currently under debate how electronic correlations influence the critical behavior of a collective QPT.^{15,16} With this in mind, in this work, we show how incorporation of interorbital charge and spin fluctuations introduces a coherent superposition of local electronic states (multiparticle entanglement) characteristic of PAM¹¹ and related (Kondo) models.¹² We explore the evolution of charge gaps and the correlated nature of the orbital states in this quantum regime, providing a way to visualize the dynamical nature of an orbital entangled state and how it is created in periodic systems governed by strong electron-electron interactions.

II. EXTENDED MODEL AND SOLUTION

The combined version of the PAM and FKM first introduced in the context of mixed valence compounds⁴ reads

$$H = - \sum_{ij,\sigma} t_{ij} d_{i\sigma}^\dagger d_{j\sigma} - \mu \sum_{i,\sigma} (n_{i\sigma}^d + n_{i\sigma}^f) + E_f \sum_{i,\sigma} n_{i\sigma}^f + U_{ff} \sum_i n_{i\uparrow}^f n_{i\downarrow}^f + V \sum_{i,\sigma} (d_{i\sigma}^\dagger f_{i\sigma} + f_{i\sigma}^\dagger d_{i\sigma}) + U_{df} \sum_{i,\sigma\sigma'} n_{i\sigma}^d n_{i\sigma'}^f. \quad (1)$$

Here, $d_{i\sigma}^\dagger$ ($f_{i\sigma}^\dagger$) is the creation operator for the conduction (localized) electrons of spin σ at site i . t_{ij} is the hopping matrix element between sites i and j , E_f is the f -electron on-site energy, and μ is the chemical potential, which preserves the total number of electrons $n_{tot} = \sum_{\sigma} \langle n_{\sigma}^d \rangle + \langle n_{\sigma}^f \rangle$ at each lattice site.

This model accounts for the nontrivial effects arising from the interplay between the interorbital electron-electron interactions U_{df} and the hybridization V . The role of these two

competing terms in the dynamical charge fluctuations in the Kondo lattices was recently addressed within the numerical renormalization group formalism.¹⁷ The two-orbital Hamiltonian H [Eq. (1)] was further generalized by including the on-site Coulomb interaction in the conduction band U_{dd} along with the Hund coupling J_H .^{18,19} Interestingly, at half-filling, a transition between the Mott-Hubbard and the Kondo insulating states was found in Ref. 19. However, to the best of our knowledge, the role of orbital rehybridization in generating quantum local (fd) entanglement¹¹ has not been investigated to date. To highlight the dynamical nature of this quantum state, we study the one-particle spectra in a regime where the f shell is half-occupied and the conduction band is both half- and partially filled. The *extended* periodic Anderson model (ePAM) considered here is given by

$$\bar{H} = H + E_d \sum_{i,\sigma} n_{i\sigma}^d + U_{dd} \sum_i n_{i1}^d n_{i1}^d. \quad (2)$$

In this work, we study the effect of electronic interactions in the one-particle spectra of ePAM at $T=0$ on a hypercubic lattice, where the bare electronic density of states (DOS) becomes $\rho_0(\epsilon) = \frac{1}{\sqrt{\pi t^*}} \exp[-\frac{\epsilon^2}{t^{*2}}]$,²⁰ with $t^*=1$ being the energy unit. We will consider both the half-filled case, where all bands are centered with respect to the Fermi level $\omega=0$, as well as a (valence) regime where the filling of the conduction band is fixed to $\langle n_d \rangle = 0.8$.²¹

We focus on the Kondo regime where the Coulomb interactions are not too strong and comparable to the strength of the on-site hybridization V and the width of the conduction band.¹⁹ With this choice, we shall underline the origin of an orbital entangled state in Eq. (2), providing a theoretical basis for future investigations on the electronic properties of materials where localized electrons [characteristic of heavy-fermion systems where the direct (ff) hopping is small] interact with narrow conduction bands. This class of materials includes, for example, Ce- (Ref. 22) and Eu-based²³ compounds as well as GdI_2 .²⁴ The latter is the prototype material where $5d_{z^2}$ conduction electrons are strongly scattered by localized $4f^7$ electrons. Also, of great interest in the context of Eq. (2) are materials where both the localized electrons and the electrons forming the conduction band carry large magnetic moment,²⁵ not to exclude multichannel solid-state structures.^{26,27}

To treat the dynamical effects of the strong intraorbital Coulomb interactions and multiple-scattering processes produced by moderately strong, interorbital repulsions, we use the dynamical-mean-field theory (DMFT)¹⁰ as an approximation to our ePAM problem [Eq. (2)]. The DMFT solution involves replacing the lattice model by a self-consistently embedded (asymmetric) Anderson impurity model and a self-consistency condition requiring the local impurity Green's function to be equal to the local propagator for the lattice. Similar to what is obtained for the regular PAM,²¹ at high dimensions, the local (f, d) propagators of ePAM are written as

$$G_{ii,\sigma}^d(\omega) = \tilde{D} \left(\xi_{\sigma}^d(\omega) - \frac{V^2}{\xi_{\sigma}^f(\omega)} \right), \quad (3)$$

and

$$G_{ii,\sigma}^f(\omega) = \frac{1}{\xi_{\sigma}^f(\omega)} \left[1 + \frac{V^2}{\xi_{\sigma}^d(\omega)} G_{ii,\sigma}^d(\omega) \right], \quad (4)$$

where $\xi_{\sigma}^{\alpha}(\omega) \equiv \omega + \mu - E_{\alpha} - \Sigma_{\sigma}^{\alpha}(\omega)$ ($\alpha=f, d$) and $\tilde{D}(z) \equiv \int d\epsilon \frac{\rho_0(\epsilon)}{z-\epsilon}$ is the Hilbert transform of $\rho_0(\epsilon)$.

In this work, we confine ourselves to the theoretical description in the paramagnetic phase of ePAM, where the Green's functions [Eqs. (3) and (4)] are computed using the following relation for the correlated self-energies:

$$\Sigma^{\alpha}(\omega) = \sum_{\beta} \left[N_{\alpha\beta} U_{\alpha\beta} \langle n^{\beta} \rangle + \frac{A_{\alpha\beta} \Sigma_{\alpha\beta}^{(2)}(\omega)}{1 - B_{\alpha\beta} \Sigma_{\alpha\beta}^{(2)}(\omega)} \right], \quad (5)$$

with $\Sigma_{\alpha\beta}^{(2)}(\omega) = N_{\alpha\beta} \frac{U_{\alpha\beta}^2}{\beta^2} \sum_{lm} G_{\alpha}^0(i\omega_l) G_{\beta}^0(i\omega_m) G_{\beta}^0(i\omega_l + i\omega_m - i\omega)$ being the second-order (in $U_{\alpha\beta}$) contributions and $N_{\alpha\beta} = 2 - \delta_{\alpha\beta}$. In contrast to usual one-band (Hubbard model, PAM, etc.) correlated problems, the atomic limit for the multi-orbital case contains local, interorbital correlation functions, $D_{\alpha\beta}$.²⁸ The equations for the parameters $A_{\alpha\beta}$ and $B_{\alpha\beta}$ are explicit functions of $U_{\alpha\beta}$, $D_{\alpha\beta}$, and the average numbers (per spin σ) $\langle n^{\alpha} \rangle \equiv n^{\alpha}$ and $\langle n_{\alpha}^0 \rangle$.²⁹ The latter is the *effective* number of fermions in the α orbital corresponding to site-excluded Green's function $G_{\alpha}^0(\omega)$ [with $[G_{\alpha}^0(\omega)]^{-1} \equiv [G_{ii}^{\alpha}(\omega)]^{-1} + \Sigma^{\alpha}(\omega)$]. The above relations form a closed set of coupled, nonlinear equations which are solved numerically until convergence is achieved.

The two-orbital iterated perturbation theory (IPT) [Eq. (5)] is a multi-orbital interpolative ansatz that connects the two exactly soluble limits of the one-band Hubbard model (HM) and the PAM model, namely, the uncorrelated ($U_{\alpha\beta} = 0$) and the atomic ($\epsilon_{\mathbf{k}}^d = 0$) limits. It accounts for the correct low- and high-energy behavior of the one-particle spectra (see below) and the correlated Fermi liquid (FL) behavior for the f electrons of PAM³⁰ and the conduction band of the HM³¹ in the large- D limit. Finally, for HM, it ensures the Mott-Hubbard metal-insulator transition from a correlated FL metal to a Mott-Hubbard insulator as a function of the Coulomb interaction U_{dd} .¹⁰ As shown below, the DMFT (IPT) solution introduces nontrivial effects stemming from the dynamical nature of the strong electronic correlations. Namely, these processes lead to large transfer of spectral weight across large energy scales in response to small changes in the electronic parameters, a characteristic lying at the heart of the anomalous responses of correlated systems.

III. RESULTS AND DISCUSSION

We now present our results. Let us begin with the regular PAM. In Fig. 1, we show the corresponding one-particle DOS for $U_{ff}=2$, $V=0.6$,³² and two distinct band fillings for the conduction band. The f -electron DOS obtained at half-filling $n_{\sigma}^f = n_{\sigma}^d = 0.5$ is in very good agreement with numerical quantum Monte Carlo (QMC) results for the same model.³² The charge gap at the Fermi level (E_F), the width of the Kondo resonance, as well as the position of the incoherent (Hubbard) bands near $\omega = \pm 2$ are all well accounted for by the IPT solver. We also perform calculations for $n_{\sigma}^d = 0.4$ and $n_{\sigma}^f = 0.5$, where IPT results were proved to be in agreement

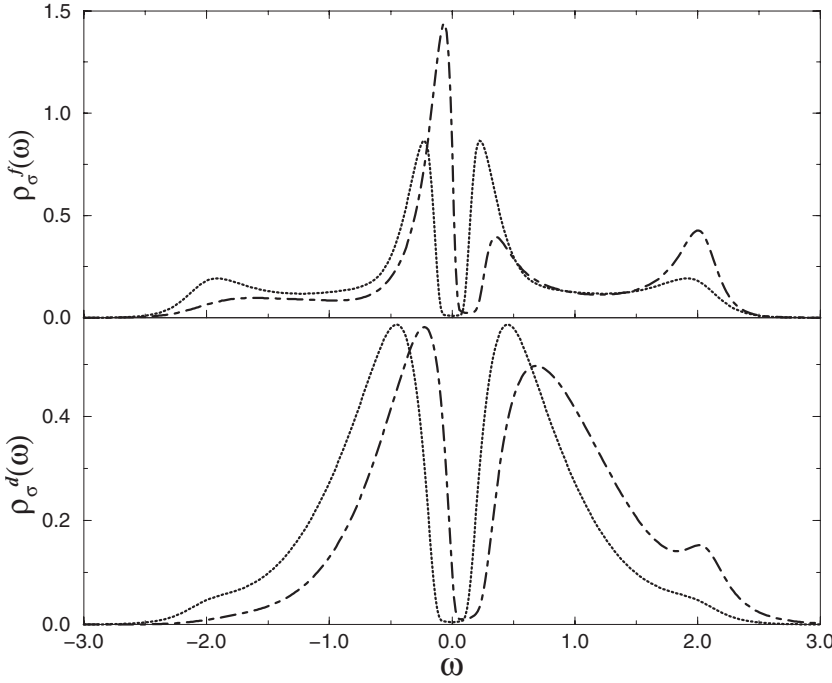


FIG. 1. $T=0$ orbital resolved density of states (f -upper and d -lower panels) for the periodic Anderson model (PAM) with fixed $U_{ff}=2$, $V=0.6$, $n_{\sigma}^f=0.5$, and two fillings for the conduction band: $n_{\sigma}^d=0.5$ (dotted line) and $n_{\sigma}^d=0.4$ (dot-dashed line). Notice the band-gap characteristic of PAM in both channels.

with QMC calculations.²¹ Following the usual practice, the band filling is achieved by adjusting self-consistently the chemical potential μ and the on-site energies E_{α} . As seen in Fig. 1, a metallic state is found in the asymmetric regime (with $n_{tot}=1.8$), where the d - and f -spectral functions are finite at $\omega=0$. As in Ref. 21, we find asymmetric one-particle DOS for the f electrons in spite of its commensurate filling. In agreement with QMC results,²¹ the Kondo peak at lower binding energies increases and it is pushed toward E_F . On the other hand, its counterpart at positive frequencies is considerably reduced, with the corresponding spectral weight being transferred to the upper Hubbard band at $\omega \approx 2$. The opposite trend for the dynamical spectral weight transfer is found below E_F . Here, the one-particle spectra are transferred from the lower Hubbard band (at high binding energies) to the Kondo states near E_F . Notice that similar effects are also visible in the d -DOS; however, due to their intrinsic weakly correlated nature, the conduction electrons are clearly less affected by changes in the band filling. The dynamical transfer of spectral weight found in the asymmetric regime of PAM will be crucial for a concrete understanding of the non-trivial evolution of the many-body correlated states of the ePAM.

We now turn to the spectral properties of ePAM [Eq. (2)]. To reduce the number of free parameters of the extended model \bar{H} , we chose the same value for the intraorbital Coulomb interactions, i.e., $U_{ff}=U_{dd} \equiv U=2$. $U_{df}(<U)$ will be varied in steps to highlight the role of electron-electron interactions taking place between different orbitals. To begin with, we consider the $U_{df}=0$ limit of Eq. (2), i.e., the periodic Anderson-Hubbard model.³³ At half-filling ($\mu=0$, $E_{\alpha}=-U/2-U_{df}$),¹⁹ the d -DOS is considerably modified, while the f -DOS remains practically unchanged. This is fully consistent with Anderson's assumption¹ that the f electrons are weakly affected by electronic correlations taking place on wide conduction bands. Surprisingly, the dotted (red) line of

Figs. 2 and 3 shows that this hypothesis is valid for narrow conduction bands if U_{dd} is not too large or away from the strongly correlated Mott-Hubbard regime.¹⁹ On the other hand, the conduction band is considerably influenced by the Coulomb interaction U_{dd} . As found for the HM,¹⁰ in Fig. 2, we see the presence of Hubbard satellites and quasiparticle (Kondo-like) resonances in the d shell. Similar effects are also visible in asymmetric d -DOS of Fig. 3.

By switching on U_{df} , the f and d channels become locally *entangled* due to dynamical charge and spin fluctuations, which are proved to be well described within our scheme. These quantum fluctuations are caused by two-particle inter-orbital scattering processes (U_{df}) (see discussion below), whose effect is to reduce the coherent Kondo scale characterized by the narrowing of the f, d Kondo resonances. This is accompanied by an enhancement of the incoherent Hubbard bands. Crossing points intrinsic of correlated electron systems are visible in both channels. Correlation effects are also present in the self-energies, implying the large effective mass for the heavy electrons and the carriers in the conduction band. Our results (Figs. 2 and 3) suggest that in the limit of very large U_{df} , both channels will show similar properties, making it difficult to distinguish their intrinsic magnetic and orbital fingerprints. This entangled multi-orbital state is expected to have implications for spectroscopy (photoemission, inverse-photoemission, tunneling, and optical measurements) of real heavy-electron materials with almost half-filled bands.

The dashed lines of Fig. 3 display our results in the vicinity of a metal-insulator transition point. At $U_{df}<1$, the valence band spans the Fermi energy in the asymmetric metallic regime. As in Fig. 2, the lower and upper Hubbard bands are enhanced by U_{df} . Interesting, however, is the evolution of the Kondo resonance in the correlated (f, d) channels. Note that the strong asymmetric profile of the Kondo resonances near E_F is practically lost for $U_{df}=1.5$, indicating the formation of a multiparticle entangled state at low energies. Ac-

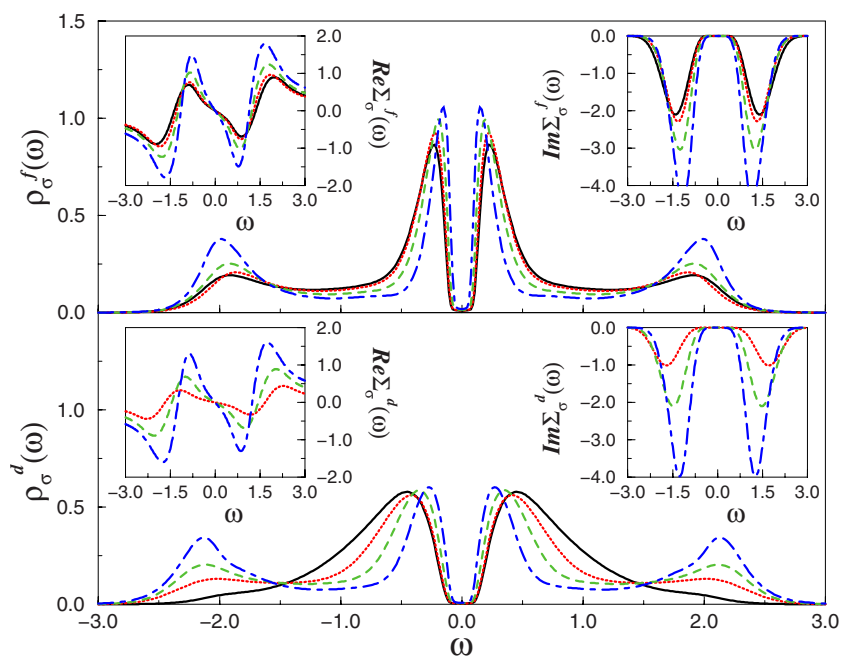


FIG. 2. (Color online) $T=0$, orbital resolved density of states, f (d) upper (lower) panel, of the extended periodic Anderson model (ePAM) for $n_{\sigma}^f=n_{\sigma}^d=0.5$, $U_{ff}=U_{dd}=2$, $V=0.6$, and three values of U_{df} : $U_{df}=0$ (dotted line), $U_{df}=1.0$ (dashed line), and $U_{df}=1.5$ (dot-dashed line). [Our results for regular PAM (solid line) are plotted for comparison.] The corresponding real (left) and imaginary (right) parts of the self-energies are shown in the insets. Notice the enhancement of the Hubbard bands and the narrowing of the Kondo resonance with increasing U_{df} . This is the fingerprint of dynamical multiparticle entanglement, whose correlation effects are encoded in the self-energies.

According to our results, strong local fd entanglement¹¹ restores the particle-hole symmetry of the Kondo screening cloud, driving the system into a continuous metal-insulator transition. Thus, the anomalous response shown in Fig. 3 appears to be correlated with the proximity to a localization-delocalization transition in ePAM and could have implications for critical QPTs in rare-earth compounds.³⁴

The $T=0$ DOS of Fig. 3 shows that entangled (fd) quasiparticles are formed at low energies in the asymmetric insulating regime of ePAM. As seen in this figure, the insulating state results from a delicate interplay between correlation-induced low- and high-energy scattering processes taken place in the upper d band. These, in turn, drive large spectral weight transfer from intermediate ($0.5 \leq \omega \leq 1.5$) to higher energies $\omega \approx 2$. Given the profound similarities between the

two (f, d) Kondo screening clouds, we argue that the $U_{df}=1.5$ Kondo insulating state is driven by dynamical orbital rehybridization³⁵ which strongly enhances the low-energy coherent scattering processes. This quantum effect might be relevant in understanding the correlated nature of multichannel quantum fluctuations,³⁶ where orbital, charge, and spin^{27,29,37} degrees of freedom are dynamically affected by the competition between orbital dependent one-electron hopping, orbital splittings, and electron-electron interactions.

Finally, the continuous enhancement of the many-particle Kondo resonance can be used to understand the physical origin of orbital entanglement in ePAM and related models. We notice that our results away from half-filling are complementary to those reported in Ref. 11. There it is found that by reducing the number of electrons, the fd entanglement is

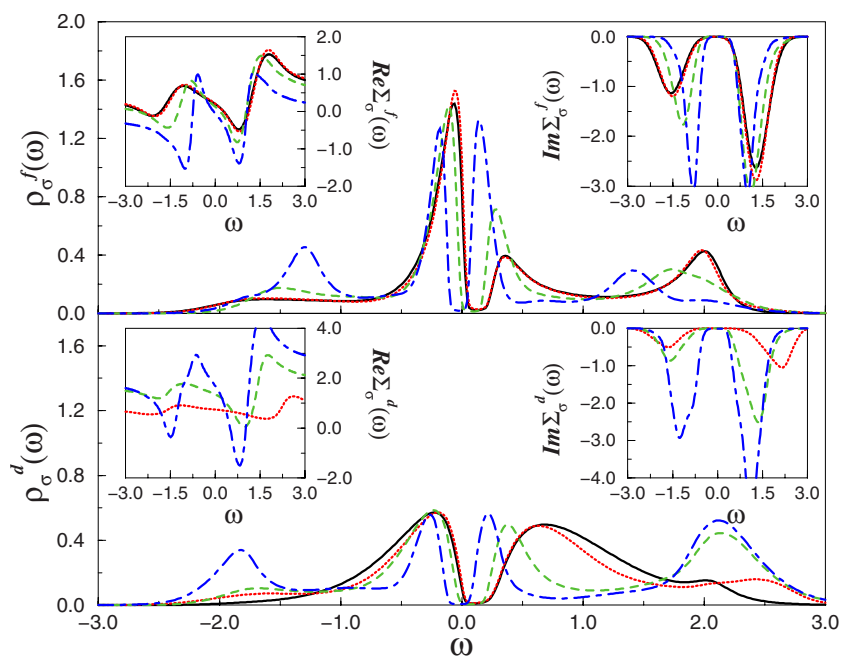


FIG. 3. (Color online) Orbital resolved density of states at $T=0$, with $n_{\sigma}^f=0.5$ and $n_{\sigma}^d=0.4$. We use the same parameters as in Fig. 2, i.e., $U_{ff}=U_{dd}=2$, $V=0.6$, $U_{df}=0$ (dotted line), $U_{df}=1.0$ (dashed line), and $U_{df}=1.5$ (dot-dashed line). The insets show the real (left) and imaginary (right) parts of the self-energies. Notice the evolution of the low-lying entangled electronic states across the continuous metal-insulator transition.

monotonically suppressed due to an *incomplete local Kondo screening*. As shown in Fig. 3, U_{df} restores the particle-hole symmetry of the Kondo screening cloud near E_F in both channels. This, in turn, controls the formation of (df) orbital singlets, explaining the relation between orbital Kondo effect²⁹ and local orbital entanglement. Our results call for extensions of the DMFT treatment in order to quantify the average and the variance of local and nonlocal concurrences (the standard measurements of quantum entanglement) in a way similar to what has been proposed on a recent study addressing the formation of quantum entanglement in the Anderson clusters.¹¹

IV. CONCLUSION

In summary, we have studied the evolution of the one-particle spectra of the ePAM using a two-orbital DMFT scheme, providing a basis for future investigations of the electronic properties of narrow-band materials. Consistent with the Falicov-Kimball ideas, it is shown that interorbital

electron interactions strongly modify the correlated spectra. We have found a route toward a Kondo insulating state which is controlled by entangled multiorbital degrees of freedom.³⁶ Near the Kondo regime, a metal-insulator transition is shown to be nonorbital selective (both orbitals become insulating simultaneously) and continuous. This transition is driven by a correlation-induced orbital rehybridization,³⁵ which enhances the entanglement between correlated channels. We clarify the formation of a coherent orbital entangled state near the Fermi energy, demonstrating the role of charge and spin fluctuations as a mechanism for (local-) orbital-Kondo entanglement. Our description is expected to have a wider application in multiorbital systems^{22–25,27} where the degrees of freedom of individual electrons in concert with electronic correlations determine the nature of quantum fluctuations.

ACKNOWLEDGMENT

This work was supported by the Emmy Noether-Programme of the DFG.

-
- ¹P. W. Anderson, Phys. Rev. **124**, 41 (1961).
²L. M. Falicov and J. C. Kimball, Phys. Rev. Lett. **22**, 997 (1969).
³P. S. Riseborough, Adv. Phys. **49**, 257 (2000).
⁴R. M. Martin and J. W. Allen, J. Appl. Phys. **50**, 7561 (1979).
⁵J. M. Lawrence, P. S. Riseborough, and R. D. Parks, Rep. Prog. Phys. **44**, 1 (1981).
⁶D. I. Khomskii and A. N. Kochargan, Solid State Commun. **18**, 985 (1976); J. W. Schweitzer, Phys. Rev. B **17**, 758 (1978).
⁷A. V. Goltsev and G. Bruls, Phys. Rev. B **63**, 155109 (2001).
⁸J. K. Freericks and V. Zlatić, Rev. Mod. Phys. **75**, 1333 (2003).
⁹A. C. Hewson, *The Kondo Problem of Heavy Fermions* (Cambridge University Press, Cambridge, 1993).
¹⁰A. Georges, G. Kotliar, W. Krauth, and M. J. Rozenberg, Rev. Mod. Phys. **68**, 13 (1996).
¹¹P. Samuelsson and C. Verdozzi, Phys. Rev. B **75**, 132405 (2007).
¹²S. Y. Cho and R. H. McKenzie, Phys. Rev. A **73**, 012109 (2006); S. Oh and J. Kim, Phys. Rev. B **73**, 052407 (2006).
¹³A. Ramšak, I. Sega, and J. H. Jefferson, Phys. Rev. A **74**, 010304(R) (2006).
¹⁴M. Nielsen and I. Chuang, *Quantum Computation and Quantum Information* (Cambridge University Press, Cambridge, 2000); see also G. Burkard, J. Phys.: Condens. Matter **19**, 233202 (2007), and references therein.
¹⁵S.-J. Gu, S.-S. Deng, Y.-Q. Li, and H.-Q. Lin, Phys. Rev. Lett. **93**, 086402 (2004).
¹⁶D. Larsson and H. Johannesson, Phys. Rev. Lett. **95**, 196406 (2005).
¹⁷A. K. Zhuravlev, V. Yu. Irkhin, and M. I. Katsnelson, Eur. Phys. J. B **55**, 377 (2007).
¹⁸K. Kubo and D. S. Hirashima, J. Phys. Soc. Jpn. **68**, 2317 (1999); S. Yotsuhashi, H. Kusunose, and K. Miyake, *ibid.* **70**, 186 (2001).
¹⁹A. Koga, N. Kawakami, R. Peters, and T. Pruschke, Phys. Rev. B **77**, 045120 (2008).
²⁰E. Müller-Hartmann, Z. Phys. B: Condens. Matter **74**, 507 (1989).
²¹N. S. Vidhyadhiraja, A. N. Tahvildar-Zadeh, M. Jarrell, and H. R. Krishnamurthy, Europhys. Lett. **49**, 459 (2000).
²²D. Purdie, M. Garnier, K. Breuer, M. Hengsberger, Y. Baer, G. Panaccione, G. Indlekofer, and C. Grupp, Solid State Commun. **106**, 799 (1998); S.-H. Yang, S.-J. Oh, H.-D. Kim, R.-J. Jung, A. Sekiyama, T. Iwasaki, S. Suga, Y. Saitoh, E.-J. Cho, and J.-G. Park, Phys. Rev. B **61**, R13329 (2000); E.-J. Cho, R.-J. Jung, B.-H. Choi, S.-J. Oh, T. Iwasaki, A. Sekiyama, S. Imada, S. Suga, T. Muro, J.-G. Park, and Y. S. Kwon, *ibid.* **67**, 155107 (2003).
²³D. Ehm, F. Reinert, G. Nicolay, S. Schmidt, S. Hüfner, R. Claessen, V. Eyert, and C. Geibel, Phys. Rev. B **64**, 235104 (2001); K. Yamamoto, K. Horiba, M. Taguchi, M. Matsunami, N. Kamakura, A. Chainani, Y. Takata, K. Mimura, M. Shiga, H. Wada, Y. Senba, H. Ohashi, and S. Shin, *ibid.* **72**, 161101(R) (2005).
²⁴C. Felser, K. Ahn, R. K. Kremer, R. Seshadri, and A. Simon, J. Solid State Chem. **147**, 19 (1999); see also I. Eremin, P. Thalmeier, P. Fulde, R. K. Kremer, K. Ahn, and A. Simon, Phys. Rev. B **64**, 064425 (2001).
²⁵N. N. Delyagin and V. I. Krylov, J. Phys.: Condens. Matter **19**, 086205 (2007).
²⁶M.-S. Choi, Rosa López, and Ramón Aguado, Phys. Rev. Lett. **95**, 067204 (2005).
²⁷P. Jarillo-Herrero, J. Kong, H. S. J. van der Zant, C. Dekker, L. P. Kouwenhoven, and S. de Franceschi, Nature (London) **434**, 484 (2005).
²⁸P. Pou, R. Pérez, F. Flores, A. Levy Yeyati, A. Martín-Rodero, J. M. Blanco, F. J. García-Vidal, and J. Ortega, Phys. Rev. B **62**, 4309 (2000).
²⁹L. Craco, M. S. Laad, and E. Müller-Hartmann, Phys. Rev. Lett. **90**, 237203 (2003).
³⁰L. Craco, J. Phys.: Condens. Matter **11**, 8689 (1999).

- ³¹M. S. Laad, L. Craco, and E. Müller-Hartmann, *Phys. Rev. B* **64**, 195114 (2001).
- ³²M. Jarrell, H. Akhlaghpour, and Th. Pruschke, *Phys. Rev. Lett.* **70**, 1670 (1993).
- ³³K. Itai and P. Fazekas, *Phys. Rev. B* **54**, R752 (1996).
- ³⁴Q. Si, S. Rabello, K. Ingersent, and J. L. Smith, *Nature (London)* **413**, 804 (2001).
- ³⁵C. A. Marianetti, G. Kotliar, and G. Ceder, *Phys. Rev. Lett.* **92**, 196405 (2004).
- ³⁶A. M. Oleś, P. Horsch, L. F. Feiner, and G. Khaliullin, *Phys. Rev. Lett.* **96**, 147205 (2006).
- ³⁷N. B. Christensen, H. M. Ronnow, D. F. McMorrow, A. Harrison, T. G. Perring, M. Enderle, R. Coldea, L. P. Regnault, and G. Aeppli, *Proc. Natl. Acad. Sci. U.S.A.* **104**, 15264 (2007).